

# Excess Protein Synthesis in FXS Patient Lymphoblastoid Cells Can Be Rescued with a p110 $\beta$ -Selective Inhibitor

Christina Gross<sup>1,3</sup> and Gary J Bassell<sup>1,2,3</sup>

Departments of <sup>1</sup>Cell Biology, <sup>2</sup>Neurology and <sup>3</sup>Center for Translational Social Neuroscience, Emory University School of Medicine, Atlanta, Georgia, United States of America

The fragile X mental retardation protein (FMRP) plays a key role for neurotransmitter-mediated signaling upstream of neuronal protein synthesis. Functional loss of FMRP causes the inherited intellectual disability fragile X syndrome (FXS), and leads to increased and stimulus-insensitive neuronal protein synthesis in FXS animal models. Previous studies suggested that excess protein synthesis mediated by dysregulated signal transduction contributes to the majority of neurological defects in FXS, and might be a promising target for therapeutic strategies in patients. However, possible impairments in receptor-dependent protein synthesis have not been evaluated in patient cells so far. Using quantitative fluorescent metabolic labeling, we demonstrate that protein synthesis is exaggerated and cannot be further increased by cytokine stimulation in human fragile X lymphoblastoid cells. Our previous work suggested that loss of FMRP-mediated regulation of protein expression and enzymatic function of the PI3K catalytic subunit p110 $\beta$  contributes to dysregulated protein synthesis in a mouse model of FXS. Here, we demonstrate that these molecular mechanisms are recapitulated in FXS patient cells. Furthermore, we show that treatment with a p110 $\beta$ -selective antagonist rescues excess protein synthesis in synaptoneurosomes from an FXS mouse model and in patient cells. Our work suggests that dysregulated protein synthesis and PI3K activity in patient cells might be suitable biomarkers to quantify the efficacy of drugs to ameliorate molecular mechanisms underlying FXS, and could be used for drug screens to refine treatment strategies for individual patients. Moreover, we provide rationale to pursue p110 $\beta$ -targeting treatments as potential therapy in FXS, and possibly other autism spectrum disorders.

Online address: <http://www.molmed.org>

doi: 10.2119/molmed.2011.00363

## INTRODUCTION

Fragile X syndrome (FXS), the most common inherited intellectual disability, is caused by loss of function of the fragile X mental retardation protein (FMRP). The analysis of animal models has shown that absence of FMRP causes pathological changes in the regulation of basal and stimulus-induced protein synthesis in the brain (1–4). These changes in neuronal protein expression are believed to underlie or contribute to

most of the neuronal dysfunctions observed in FXS (5). FMRP is an mRNA binding protein shown to regulate translation, localization and stability of many target mRNAs (6). FMRP influences the expression of members of several different protein families, such as scaffolding proteins or proteins involved in receptor trafficking. However, evidence is emerging that FMRP has a major function in regulating neurotransmitter-induced signal transduction

upstream of protein synthesis, which might cause the aberrant protein synthesis observed in the absence of FMRP (1,3,4,7–9). Pharmacological inhibition or genetic reduction of a few signal transduction pathways regulating protein synthesis, such as group 1 metabotropic glutamate receptors (mGlu<sub>1/5</sub>), glycogen synthase kinase 3 (GSK3), extracellular signal regulated kinase 1/2 (ERK1/2) and phosphoinositide-3 kinase (PI3K), were shown to rescue aberrant protein synthesis and several protein synthesis-dependent phenotypes in FXS mice [reviewed in (10,11)]. Of note, treatment with two different protein synthesis inhibitors rescued cognitive impairments in a *Drosophila* model for FXS (12). Taken together, these studies suggest that correcting dysregulated protein synthesis or defective signaling pathways regulating protein synthesis might be a promising therapeutic strategy for patients with FXS, and provided rationale

---

**Address correspondence to** Christina Gross, Department of Cell Biology, Whitehead Biomedical Research Bld. #415, Emory University School of Medicine, 615 Michael Street, Atlanta, GA 30322. Phone: 404-727-0668; E-mail: [cgross3@emory.edu](mailto:cgross3@emory.edu); or Gary Bassell, Departments of Cell Biology and Neurology, Whitehead Biomedical Research Bld. #415, Emory University School of Medicine, 615 Michael Street, Atlanta, GA 30322. Phone: 404-727-3772; Fax: 404-727-0570; E-mail: [gary.bassell@emory.edu](mailto:gary.bassell@emory.edu).  
Submitted September 25, 2011; Accepted for publication December 5, 2011; Epub ([www.molmed.org](http://www.molmed.org)) ahead of print December 7, 2011.

for the initiation of several clinical trials [reviewed in (10)].

A major challenge of current FXS research is to refine and improve treatment strategies by identification of more specific and effective drugs that target the underlying pathomechanisms. Basic research in FXS animal models that further elucidates the molecular mechanisms regulated by FMRP could help to identify more potent drugs. In addition, drug screens in easily obtainable peripheral patient cells measuring FXS-specific biomarkers would accelerate the identification of even more efficient therapies, which might differ for individual patients (13). An assay quantifying ERK1/2 activation kinetics has been suggested and used as a biomarker in FXS clinical trials, however, the underlying mechanisms of the detected ERK1/2 dysfunctions are not fully understood (14–16). Studies in *Fmr1* knockout (KO) mice suggest that the ERK1/2 pathway is hypersensitive to receptor activation, but the precise mechanisms remain obscure (1).

So far, there are no biochemical cell-based assays available that quantify a molecular function shown to be directly regulated by FMRP, and thus could be used in drug screens. Such assays would also be crucial to evaluate whether a drug used in a clinical trial for FXS ameliorates underlying molecular defects.

We have shown recently that FMRP regulates the mRNA translation and protein expression of the PI3K catalytic subunit p110 $\beta$ , leading to excess PI3K activity, downstream signaling and protein synthesis in *Fmr1* KO mice (3). Excess p110 $\beta$  expression and activity could also be detected in cultured nonneuronal cells treated with siRNA to knock-down FMRP, implying that the molecular pathomechanism is not neuron specific. A broad spectrum PI3K inhibitor rescued several phenotypes in the mouse model (3). Based on these previous observations, we hypothesized that reduction of p110 $\beta$  subunit-specific PI3K activity might be an efficient therapeutic strategy in FXS and that the underlying molecular mechanism might be

detectable in peripheral cells, such as lymphoblastoid cell lines from humans with FXS.

Here, using a quantitative and scalable fluorescent metabolic labeling assay, we show that protein synthesis rates are increased and dysregulated in FXS patient lymphoblastoid cells. We provide evidence suggesting that the underlying mechanisms observed in neurons, that is, increased p110 $\beta$  protein expression, excess p110 $\beta$ -specific PI3K activity and downstream signaling are recapitulated in patient nonneuronal cells. Furthermore, we show that a p110 $\beta$ -selective antagonist rescues excess protein synthesis in synaptic fractions from *Fmr1* KO mice and in FXS patient lymphoblastoid cells, providing rationale for p110 $\beta$ -selective inhibition as potential novel therapeutic strategy for FXS. Moreover, our results suggest that, in the future, similar assays quantifying excessive protein synthesis might be suitable to screen for drugs targeting FXS-underlying pathomechanisms.

## MATERIALS AND METHODS

### Drugs and Antibodies

TXG-221 (Selleck Chemicals, Boston, MA, USA) was dissolved in dimethyl sulfoxide (DMSO) (5 mmol/L). Human interleukin (IL)-2 (PeproTech, Rocky Hill, NJ, USA) was dissolved in 0.02 N HCl (10<sup>6</sup> units/mL). Anisomycin (Sigma-Aldrich, St. Louis, MO, USA) was dissolved in DMSO (25 mmol/L). phospho-Akt, Akt, phosphoS6 and S6 antibodies were purchased from Cell Signaling Technologies (Danvers, MA, USA), p110 $\beta$  antibody for Western blotting was purchased from Santa Cruz Biotechnologies (Santa Cruz, CA, USA), p110 $\beta$  antibody for immunoprecipitation was purchased from Millipore (Billerica, MA, USA). Tubulin antibody for Western blotting was purchased from Sigma-Aldrich, the  $\beta$ -tubulin antibody for immunocytochemistry was purchased from Developmental Studies Hybridoma Bank (University of Iowa, Iowa City, IA, USA). The Cy2-coupled anti-mouse secondary anti-

body was purchased from Jackson ImmunoResearch Laboratories (West Grove, PA, USA).

### Mice and Tissue Preparation

Male *Fmr1* KO mice in C57BL/6J background and male wild-type (WT) littermates (The Jackson Laboratory, Bar Harbor, MA, USA) were used at postnatal d 17–20. Synaptoneurosomes (SNS) were prepared as described previously (4). The animal protocol was approved by the Institutional Animal Care and Use Committee, Emory University, and complied with the *Guide for the Care and Use of Laboratory Animals* (17).

### Lymphoblastoid Cell Lines and Cell Culture

Epstein-Barr virus (EBV)-transformed lymphoblastoid cell lines (LCLs) from healthy controls (GM10851: male, Caucasian, 52 years, unaffected [Coriell Institute, Camden, NJ, USA], called “Ctr”; J1: male, unaffected [18], called “Ctr-b”), and FXS (GM03200: male, Caucasian, 34 years, hypermethylated CGG repeat expansion, affected [Coriell Institute], called “FXS”; DM316: male, Caucasian, 3 years, nucleotide deletion within the *FMR1* gene, affected [19,20], called “Fdel”) patients were cultured in RPMI supplemented with 10% fetal bovine serum and antibiotics at 37°C and 5% CO<sub>2</sub> (cell density ~500,000 cells/mL).

### Radioactive PI3K Assays

Synaptoneurosomes (SNS) from one mouse cortex or 1–2 million LCLs, respectively, were used per experiment. LCLs were washed once with ice-cold PBS, and lysed in ice-cold PI3K assay lysis buffer (50 mmol/L Tris-HCl, pH 7.4, 40 mmol/L NaCl, 1 mmol/L EDTA, 0.5% Triton X-100, 1.5 mmol/L Na<sub>3</sub>VO<sub>4</sub>, 50 mmol/L NaF, 10 mmol/L sodium pyrophosphate, and 10 mmol/L sodiumglycerol phosphate, supplemented with proteinase inhibitors). SNS were lysed as described previously (3). 100  $\mu$ g protein was used for subsequent immunoprecipitation with a p110 $\beta$ -specific antibody. PI3K activity assays and thin-layer chro-

matography were performed as described previously (3,21).

### ELISA PI3K Assays

PI3K activity enzyme-linked immunosorbent assays (PI3-Kinase Activity ELISA: Pico, Echelon Biosciences, Inc, Salt Lake City, UT, USA) were performed with p110 $\beta$  protein immunoprecipitated from SNS or LCLs (as above), following the manufacturer's instructions, with these modifications: kinase reactions were conducted in 60  $\mu$ L volume with 75  $\mu$ mol/L adenosine triphosphate (ATP), 1 mmol/L dithiothreitol (DTT) and 15  $\mu$ mol/L phosphatidylinositol (3,4) biphosphate diC<sub>8</sub> for 3 h. Reactions were stopped with 2.4 mmol/L ethylenediaminetetraacetic acid (EDTA). A standard curve was used to quantify the amount of phosphatidylinositol (3,4,5) triphosphate present after the reaction.

### PhosphoS6 and S6-Specific ELISAs

Equal amounts of protein were analyzed for phosphoS6 and S6 protein levels using PathScan<sup>®</sup> phosphoS6 or total S6 ribosomal protein sandwich ELISA antibody pairs, respectively, according to the manufacturer's protocol (Cell Signaling Technology). Ratios of phosphoS6 and S6 in the same samples were compared and quantified.

### Metabolic Labeling in SNS

Metabolic labeling in SNS was performed as described previously (3,4). Where indicated, SNS were incubated for 10 min with 1  $\mu$ mol/L TGX-221 or an equal amount of dimethyl sulfoxide (DMSO) before labeling.

### Bioorthogonal Labeling and Click-iT<sup>®</sup> Chemistry

Bioorthogonal labeling in LCLs and subsequent Click-iT chemistry (Life Technologies Invitrogen, Carlsbad, CA, USA) were performed according to the manufacturer's protocol. Briefly, LCLs were kept for 1 h in methionine-free media. Where indicated, TGX-221 or anisomycin was added to the methionine-free medium after 30 min, or IL-2 was added

after 45 min. Cells were pulsed with 50  $\mu$ mol/L L-azidohomoalanine for a total time of 1 h. After 45 min, cells were plated on poly-lysine-coated coverslips, washed once with PBS 15 min after plating, and fixed with 4% paraformaldehyde. Click-iT reaction was performed as described in the manual with 5  $\mu$ mol/L tetramethylrhodamine (TAMRA) alkyne. Cells were further processed for immunocytochemistry with a  $\beta$ -tubulin antibody and a Cy2-labeled secondary antibody.

### Western Blot Analysis

Sodium dodecyl sulfate polyacrylamide gel electrophoresis (SDS-PAGE), Western blotting, and densitometric analysis using ImageJ software (NIH) were performed as described previously (3,4). Signals for phospho antibodies were normalized to the signal of the respective total antibody and tubulin on the same blot, p110 $\beta$ -, p110 $\alpha$ -, p110 $\delta$ - and FMRP-specific signals to tubulin-specific signal on the blots.

### Image Acquisition and Analysis

Images were acquired with a wide-field fluorescent Nikon Eclipse inverted microscope equipped with a cooled charge-coupled device (CCD) camera and built-in Z-drives. Z-Stacks were deconvolved using AutoQuant X (Media Cybernetics, Bethesda, MD, USA). Fluorescent signal intensities were quantified with Imaris Software (Bitplane, Zurich, Switzerland). Total fluorescent intensities for both channels were background subtracted and measured for the entire stack. Background was determined as fluorescent intensity in an area of the image that did not contain cells. Approximately 15 images per condition and experiment were acquired and analyzed. Fluorescent signal intensities of newly incorporated amino acids were normalized to tubulin signal.

### Statistical Analysis

All statistical analyses were performed with PASW Statistics 18 (Armonk, NY, USA). Data were tested for normal distribution and homogeneity of variances,

and appropriate statistical tests were used as indicated. The  $\alpha$  level was 0.05 for all tests. Data in Figures 1A, 1B, 4H and 4I are presented normalized to the mean of untreated healthy control, but statistical analyses were performed on original data. All error bars represent standard error of mean (SEM).

## RESULTS

### Dysregulated Protein Synthesis in FXS Patient Lymphoblastoid Cells

A prominent phenotype of the FXS mouse model is increased and stimulus-insensitive protein synthesis, which leads to impairments of several protein synthesis-dependent forms of synaptic plasticity (5,6). To test whether dysregulated protein synthesis in the absence of FMRP can be detected in nonneuronal, peripheral cells from human patients with FXS, we quantified protein synthesis rates in lymphoblastoid cell lines (LCLs) from a healthy control (called "Ctr" in figures and legends) and a patient with FXS that carried the full mutation, that is, completely methylated trinucleotide expansion in the *FMR1* gene (subsequently called FXS cells). We chose LCLs, because they are a virtually unlimited source of patient material, and do not require an invasive biopsy. Furthermore, lymphocytes have been recognized as a valid model for cell signal transduction, because of the variety of different signaling pathways present in these cells (22). This suggests that they are especially suitable to analyze diseases like FXS that are characterized by dysregulated signal transduction. To quantify newly synthesized proteins in LCLs, we used a fluorescent metabolic labeling method (Click-iT technology, Invitrogen), which employs bioorthogonal amino acids that can be labeled with fluorescent molecules via alkyne-azide-based Click-iT chemistry (23). Here, we used a fluorophore-coupled alkyne and the bioorthogonal amino acid azidohomoalanine to visualize and quantify newly synthesized proteins. Either pretreatment with the protein synthesis inhibitor anisomycin, or

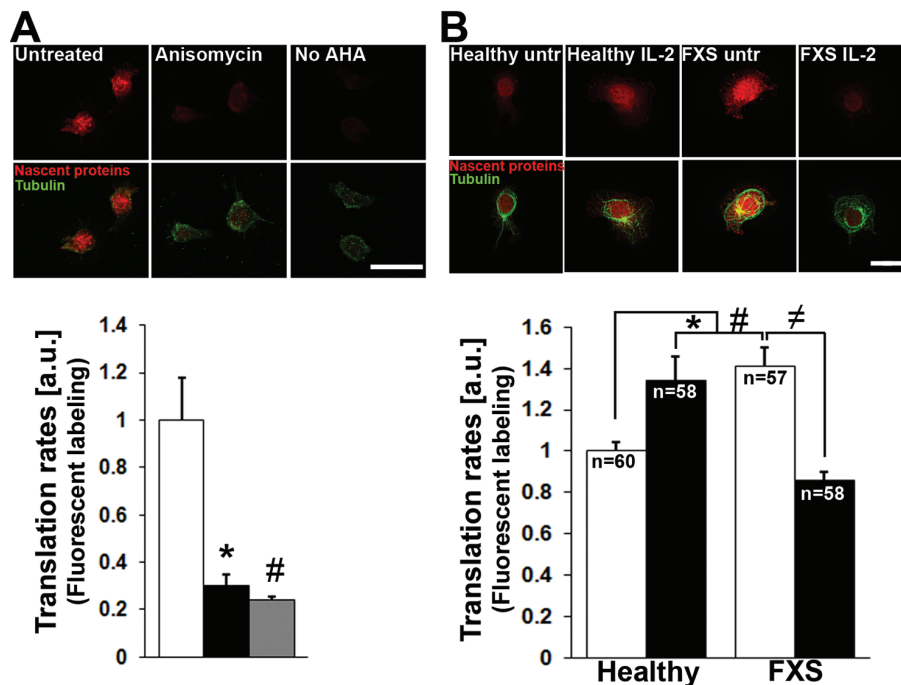


**Figure 1.** Increased and dysregulated protein synthesis in LCLs from a patient with FXS. Newly synthesized proteins in LCLs from a healthy control (Ctr: cell line GM10851) and a patient with FXS (FXS: cell line GM03200) were fluorescently labeled with Click-iT chemistry using a bioorthogonal amino acid (azidohomoalanine) and red-fluorescent tetramethylrhodamine (TAMRA) alkyne. LCLs were counterstained with a tubulin antibody for normalization of fluorescent signal (green). (A) Specificity of the fluorescent signal as an indicator of new protein synthesis is shown by strongly reduced red signal after treatment with the protein synthesis inhibitor anisomycin, and when azidohomoalanine (AHA) was omitted ( $n = 5$ ,  $*P = 0.034$ ,  $^{\#}P = 0.028$ , 1-way ANOVA with Games-Howell *post hoc* analyses). (B) Basal protein synthesis is increased and cannot be further increased by IL-2 stimulation in LCLs from FXS patients. Both control cells as well as FXS cells were stimulated with IL-2 (100 U/mL) for 30 min before labeling. In control cells, this leads to a significant increase in protein synthesis rates, whereas in FXS cells, protein synthesis rates are significantly decreased upon IL-2 treatment ( $n$  (Ctr untreated) = 60,  $n$  (Ctr IL-2) = 58,  $n$  (FXS untreated) = 57,  $n$  (FXS IL-2) = 58; 4 independent experiments, 2-way ANOVA shows significant interaction of treatment and genotype, Bonferroni *post hoc* analyses,  $*P = 0.005$ ,  $^{\#}P = 0.002$ ,  $^{\neq}P = 0.001$ ). Example images for each condition in (A, scale bar is 20  $\mu\text{m}$ ) and (B, scale bar is 10  $\mu\text{m}$ ) are shown above; upper panel: newly synthesized proteins (red), lower panel: overlay with tubulin staining (green). a.u., Arbitrary units. A:  $\square$ , Untreated;  $\blacksquare$ , anisomycin;  $\blacksquare$ , no AHA; B:  $\square$ , untreated;  $\blacksquare$ , IL-2.

omitting the bioorthogonal amino acid in the reaction, significantly reduced the fluorescent intensity, indicating that the fluorescent signal indeed represented newly synthesized proteins, and was dependent on the presence of azidohomoalanine (Figure 1A,  $n = 5$ ,  $*P = 0.034$ ,  $^{\#}P = 0.028$ , 1-way analysis of variance (ANOVA) with Games-Howell *post hoc* analyses). In contrast, tubulin counterstaining was unaffected by these treatments. Using this

method, we detected increased basal protein synthesis in LCLs from a patient with FXS (Figure 1B). Furthermore, stimulation with IL-2 (100 U/mL, 15 min prior labeling), which significantly increased protein synthesis rates in control cells, did not induce protein synthesis in FXS cells, but led to significantly reduced translation rates [Figure 1B,  $n$  (Ctr untreated) = 60,  $n$  (Ctr IL-2) = 58,  $n$  (FXS untreated) = 57,  $n$  (FXS IL-2) = 58; 4 inde-

pendent experiments, 2-way ANOVA shows significant interaction of treatment and genotype, Bonferroni *post hoc* analyses,  $*P = 0.005$ ,  $^{\#}P = 0.002$ ,  $^{\neq}P = 0.001$ ]. These results suggest that FMRP regulates cell surface receptor-mediated protein synthesis in peripheral lymphocytes, leading to dysregulated protein synthesis in LCLs from FXS patients, similarly to what has been observed in neurons from *Fmr1* KO mice (1,3,4,9).

### Increased PI3K Activity and Downstream Signaling in FXS Patient Lymphoblastoid Cells

We have shown previously that excessive signaling through PI3K contributes to dysregulated protein synthesis in the absence of FMRP (3). To test whether the molecular mechanisms underlying dysregulated protein synthesis in mouse *Fmr1* KO neurons were recapitulated in LCLs from patients with FXS, we examined PI3K activity in control and FXS LCLs. Using a radioactive PI3K assay with phosphoinositide and radio-labeled ATP as substrates, we could show elevated PI3K activity in LCLs from the FXS patient. Densitometric quantification of the phosphoinositide-3-phosphate-specific signal on the autoradiographs showed significantly increased activity in the FXS LCLs compared with healthy control (Figure 2A, example autoradiography and FMRP-specific western blot in top panel, quantification of radioactive signal in lower panel:  $n = 5$ ,  $*P = 0.048$ , paired *t* test). Of note, we could also detect excess PI3K activity in the FXS LCLs using an ELISA-based colorimetric assay, which might be suitable for automated large-scale applications (Figure 2B,  $n = 5$ ,  $*P = 0.005$ , paired *t* test). We further could show that PI3K activity in LCLs from a patient with a rare deletion within the *FMR1* gene (subsequently called Fdel LCLs) was similarly increased, whereas PI3K activity in LCLs from another healthy control (subsequently called Ctr-b in figures and legends) was comparably low (Figure S1). Western blot analyses (Figure 2C and Figure S1) revealed that no FMRP was detectable in Fdel cells,

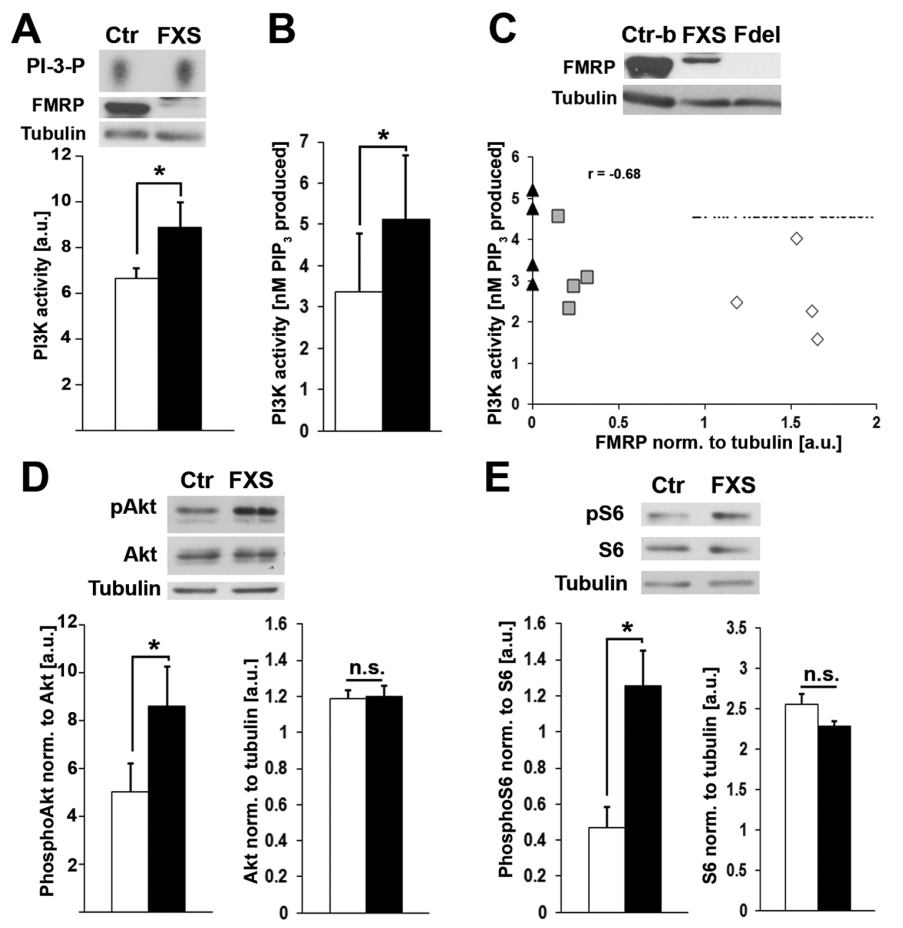


**Figure 2.** Increased PI3K activity and downstream signaling in LCLs from FXS patients. (A, B) Immunoprecipitated PI3K catalytic subunit p110 $\beta$  from LCLs shows higher PI3K enzymatic activity in FXS patient cells compared with a healthy control in two different assays. (A) PI3K activity was detected with a radioactive assay using phosphoinositide (PI) and radiolabeled ATP as substrate, followed by thin layer chromatography and autoradiography. Densitometric quantification of autoradiographies showed significantly higher PI3K activity in LCLs from a patient with a full trinucleotide expansion (FXS (■), cell line GM03200) compared with healthy control LCLs (Ctr (□), cell line GM10851) ( $n = 5$ ,  $*P = 0.048$ , paired  $t$  test). An example autoradiography and FMRP-specific Western blot analysis is shown on top. Tubulin served as loading control. Note that residual FMRP expression can be detected in the FXS LCLs. (B) Increased PI3K activity in FXS LCLs was also detected with a competitive ELISA (Echelon Biosciences, Salt Lake City, UT, USA) using PI(4,5)P $_2$  as substrate ( $n = 5$ ,  $*P = 0.005$ , paired  $t$  test). (C) PI3K activity was measured in healthy control LCLs (Ctr-b, cell line J1), LCLs from a patient with a deletion within the *FMR1* gene (Fdel, cell line DM316, no FMRP detectable by Western blot, as shown above) and the patient with a full trinucleotide expansion (FXS, same as in (A) and (B), residual FMRP levels detectable) using a competitive ELISA. PI3K activity was plotted against FMRP levels in the same lysates. Correlation analysis shows a significant negative correlation of PI3K activity with FMRP levels ( $n = 12$ , 4 samples per cell line, Spearman  $\rho = -0.68$ ,  $*P = 0.015$ ,  $\alpha = 0.05$ ). An example autoradiography of a radioactive PI3K assay for these LCLs is shown in Figure S1. (D, E) Increased activity of PI3K/mTOR downstream signaling is shown by elevated phosphorylation of Akt (D,  $n = 4$ ,  $*P = 0.01$ , paired  $t$  test) and S6 (E,  $n$  (pS6) = 5,  $n$  (S6) = 4,  $*P = 0.029$ , paired  $t$  test) in patient LCLs. Phospho-specific Western blot signals were normalized to total levels of Akt and S6, respectively. Akt and S6 levels normalized to tubulin were not significantly different in patient cells compared with healthy control cells ( $n^sP$  (Akt) = 0.50,  $n^sP$  (S6) = 0.27, paired  $t$  tests). a.u., Arbitrary units.; norm., normalized; n.s., not significant; ◊, Unaffected control; ■, *Fmr1* CGG repeat expansion; ▲, *Fmr1* nucleotide deletion.

whereas residual FMRP expression was detected in FXS cells, suggesting that reduction or absence of FMRP is causing excess PI3K activity in LCLs. Correlation analyses of PI3K activity with FMRP levels in Ctr-b, FXS and Fdel cells revealed a significant negative correlation of PI3K activity with FMRP protein levels (Figure 2C,  $n = 12$ , 4 samples from each cell line, Spearman rho correlation coefficient ( $\rho$ ) = -0.68,  $*P = 0.015$ ). Western blot analysis of phosphorylation levels of two PI3K downstream targets Akt and S6 corroborated excess PI3K signaling in the FXS LCLs, showing significantly increased phosphorylation of both Akt (Figure 2D,  $n = 4$ ,  $*P = 0.01$ , paired  $t$  test) and S6 in FXS LCLs compared with control (Figure 2E,  $n = 5$ ,  $*P = 0.029$ , paired  $t$  test). These results suggest that, as in *Fmr1* KO mouse neurons, excess PI3K activity and downstream signaling might underlie dysregulated protein synthesis in human patient cells.

### Increased Protein Expression of the PI3K Catalytic Subunit p110 $\beta$ in Fragile X Patient LCLs

We have shown previously that FMRP associates with p110 $\beta$  mRNA in mouse brain and regulates p110 $\beta$  mRNA translation and protein expression in mouse synaptic fractions and HEK293T cells. In the absence of FMRP, p110 $\beta$  mRNA translation and protein levels are increased, which might contribute to the excess PI3K activity (3). Here, we show that virtual absence of FMRP in FXS LCLs also leads to significantly increased p110 $\beta$  protein levels (Figure 3,  $n = 4$ ,  $*P = 0.002$ , paired  $t$  test). Likewise, p110 $\beta$  protein levels were increased in Fdel LCLs (Figure S2A). In contrast, protein levels of the other two class 1A PI3K catalytic subunits p110 $\alpha$  and p110 $\delta$  were not significantly changed in either patient cell line compared with healthy control (Figures S2B, C). Dysregulated expression of p110 $\beta$  might thus contribute to excess PI3K signaling in patient cells. Our data suggest that FMRP regulates similar molecular mechanisms in human LCLs as described for mouse neurons.

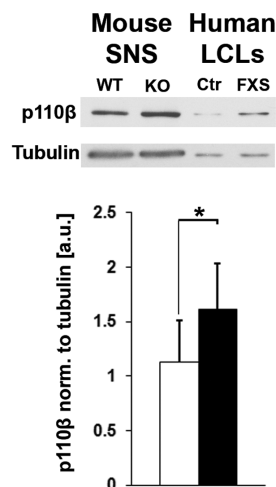


**Figure 3.** p110 $\beta$  protein expression is increased in FXS patient LCLs compared with healthy control. The increase is similar to what can be observed in synaptic fractions (SNS) from *Fmr1* KO mice (as shown previously in (3,23)). Quantification of p110 $\beta$ -specific signal normalized to tubulin in LCLs is shown in lower panel ( $n = 4$ ,  $*P = 0.002$ , paired  $t$  test). Quantification of other class 1A catalytic PI3K subunits p110 $\alpha$  and p110 $\delta$  showed no significant differences (Figure S2). a.u., Arbitrary units.; norm., normalized; □, Ctr; ■, FXS.

### A p110 $\beta$ -Selective Inhibitor Rescues Excess Protein Synthesis in *Fmr1* KO Mouse SNS and in FXS Patient LCLs

Increased and excessive p110 $\beta$ -associated PI3K activity in the absence of FMRP might underlie many of the impaired protein synthesis-dependent forms of synaptic plasticity in FXS. Based on our previous results in an FXS mouse model and our observations in human LCLs, we hypothesized that p110 $\beta$  subunit-selective PI3K antagonists might therefore be a promising disease-targeted treatment for FXS in the future. We tested this hypothesis by examining the effect of the p110 $\beta$ -selective antagonist TGX-221 (24) on excessive protein synthesis in synaptic fractions from *Fmr1* KO mice and in FXS LCLs (Figure 4). TGX-221 reduces p110 $\beta$ -specific PI3K activity and Akt phosphorylation in both WT and *Fmr1* KO SNS (1  $\mu\text{mol/L}$ , 30 min, Figure 4A).

Quantification of an ELISA-based p110 $\beta$ -specific PI3K activity assay in WT and *Fmr1* KO SNS after TGX-221 treatment shows a significant decrease in both genotypes (Figure 4B,  $n = 4$ , 2-way ANOVA, significant effect of genotype ( $*P = 0.0086$ ), and treatment ( $*P = 0.0087$ ), but no significant interaction between genotype and treatment ( $P = 0.7154$ ). Furthermore, downstream signaling is similarly reduced after TGX-221 treatment, as shown by densitometric quantification of phosphoAkt-specific Western blots [Figure 4C,  $n = 4$ , 2-way ANOVA, significant effect of treatment ( $*P = 0.0005$ ), but not genotype ( $P = 0.372$ ), and no significant interaction ( $P = 0.4894$ )]. Using metabolic labeling with radioactive methionine, we could show that protein synthesis rates were significantly reduced in *Fmr1* KO, but not WT SNS after treatment with TGX [Figure 4D,  $n = 7$ , 2-way ANOVA shows significant effect of genotype and significant interaction of treatment and genotype, LSD *post hoc* analyses,  $*P = 0.001$ ,  $\#P = 0.049$ ]. The significant interaction between genotype and treatment suggests rescue of the excess basal translation rate in FMRP deficient neurons, without adverse effects in control cells. Likewise, TGX-221 (0.5  $\mu\text{mol/L}$ , 30 min) reduced p110 $\beta$ -associated PI3K activity and S6 phosphorylation in control and FXS LCLs (Figure 4E) suggesting that TGX-221 reduces PI3K activity and downstream signal transduction regulating protein synthesis. A dose response analysis with 0.5, 1 and 5  $\mu\text{mol/L}$  TGX-221 revealed a significant, dose-dependent reduction of PI3K activity [Figure 4F,  $n = 4$ , 2-way ANOVA, significant effect of genotype ( $*P = 0.042$ ) and treatment ( $*P = 0.002$ ), but no interaction between genotype and treatment ( $P = 0.981$ )] and of S6 phosphorylation [Figure 4G, measured by ELISA,  $n = 4$ , 2-way ANOVA, significant effect of genotype ( $*P = 0.013$ ) and treatment ( $*P < 0.0001$ ), but no significant interaction between genotype and treatment ( $P = 0.195$ )]. Using bioorthogonal labeling, we could show that the p110 $\beta$ -selective

inhibitor TGX-221 significantly reduced protein synthesis rates in FXS LCLs (Figure 4H,  $n = 40$ , 4 independent experiments, 2-way ANOVA showed significant effects of genotype, treatment, and a significant interaction of genotype and treatment, Bonferroni *post hoc* analyses,  $*P = 0.001$ ,  $\#P = 0.002$ ,  $\#P = 0.021$ ). The statistically significant interaction between treatment and genotype is analogous to the results in *Fmr1* KO mice (Figure 4D), and suggests correction of excess protein synthesis in human cells from FXS patients. Repetition of the experiment using 5 and 10  $\mu\text{mol/L}$  TGX-221 showed that with these increasing concentrations of TGX-221, protein synthesis rates in FXS LCLs were fully restored to control levels [Figure 4I, 2-way ANOVA,  $*P$  (genotype) = 0.001,  $*P$  (treatment) < 0.001,  $*P$  (interaction genotype–treatment) < 0.001; Games-Howell *post hoc* analyses,  $*P = 0.001$ ,  $^{ns(1)}P = 0.966$ ,  $^{ns(2)}P = 0.999$ ]. Taken together, our results strongly suggest that excess p110 $\beta$ -specific activity contributes to dysregulated protein synthesis in both mouse *Fmr1* KO neurons and in FXS patient lymphoblastoid cells, and this hallmark disease phenotype can be corrected by a p110 $\beta$ -selective inhibitor, TGX-221.

### DISCUSSION

A major challenge for the development of disease-targeted therapeutic strategies for FXS and other cognitive and autism spectrum disorders is to provide a reliable biomarker assay that quantifies improvements in the underlying pathological mechanisms in easily accessible patient cells as an additional outcome measure for use in human clinical trials. While behavioral and cognitive tests are important to evaluate the overall benefits of the therapeutic strategy, biomarker assays targeted at the underlying molecular defects and applicable to accessible peripheral cells will help to optimize and refine drug therapies.

Our data suggest that excess protein synthesis and PI3K activity in LCLs from patients with FXS might be poten-

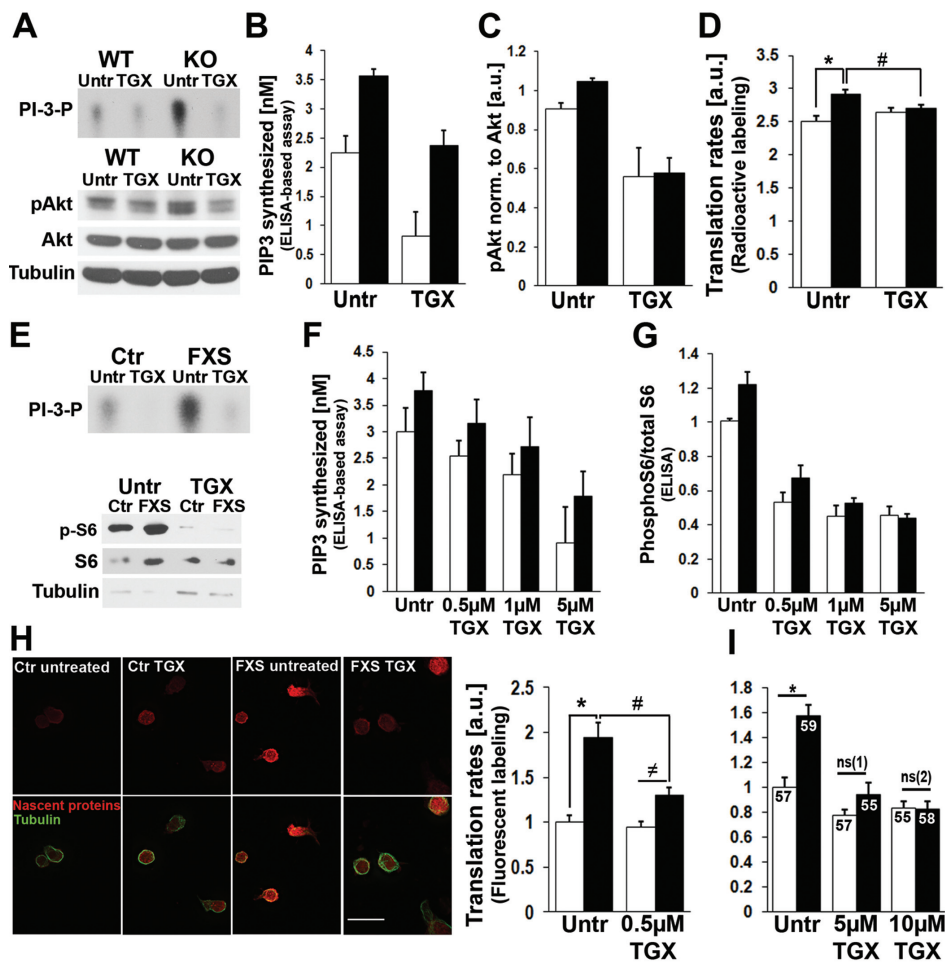


**Figure 4.** A p110 $\beta$ -selective antagonist rescues increased protein synthesis in synaptic fractions from *Fmr1* KO mice and in LCLs from a patient with FXS. (A–C) Treatment of synaptoneurosomes with TGX-221 (1  $\mu$ mol/L, 30 min) reduces p110 $\beta$ -specific PI3K activity and phosphorylation of the downstream target AKT in both WT and *Fmr1* KO SNS, shown by a radioactive PI3K assay and phosphoAkt-specific western blotting (A). (B) Quantification of PI3K activity using a competitive ELISA showed a significant reduction in PI3K activity in both genotypes after treatment ( $n = 4$ , 2-way ANOVA,  $*P$  (genotype) = 0.0086,  $*P$  (treatment) = 0.0087,  $P$  (interaction) = 0.7154). (C) Densitometric quantification of phosphoAkt-specific western blots showed a significant effect of treatment ( $C, n = 4$ , 2-way ANOVA,  $*P$  (treatment) = 0.0005,  $P$  (genotype) = 0.372,  $P$  (interaction) = 0.4894). (D) The same dose of TGX-221 (1  $\mu$ mol/L, 10 min) rescues excess protein synthesis in *Fmr1* KO SNS to WT levels as measured by metabolic labeling using radioactive methionine ( $n = 7$ , 2-way ANOVA,  $P$  (treatment) = 0.611,  $*P$  (genotype) = 0.004,  $*P$  (interaction) = 0.024; LSD *post hoc* analyses:  $*P = 0.001$ ,  $\#P = 0.049$ ). (E) TGX-221 treatment (0.5  $\mu$ mol/L, 30 min) of control and FXS LCLs reduces PI3K activity as shown by a radioactive PI3K assay of p110 $\beta$ -specific immunoprecipitates from LCL lysates, and decreases PI3K/mTOR downstream signaling as shown by strongly reduced phosphorylation of S6 independently of the genotype. (F, G) Quantification demonstrates a significant, dose-dependent effect of TGX-221 treatment on PI3K activity (F, competitive ELISA,  $n = 4$ , 2-way ANOVA,  $*P$  (genotype) = 0.0079,  $*P$  (treatment) = 0.0258,  $P$  (interaction) = 0.9418), and on S6 phosphorylation (G, ELISA,  $n = 4$ , 2-way ANOVA,  $*P$  (genotype) = 0.013,  $*P$  (treatment) < 0.0001,  $P$  (interaction) = 0.195). (H) 30-min pretreatment of LCLs with 0.5  $\mu$ mol/L TGX-221 significantly reduces protein synthesis in FXS patient cells ( $n = 40$ , 4 independent experiments, 2-way ANOVA:  $*P$  (genotype) < 0.001,  $*P$  (treatment) = 0.005,  $*P$  (interaction) < 0.001, Bonferroni *post hoc* analyses,  $*P = 0.001$ ,  $\#P = 0.002$ ,  $*P = 0.02$ ). Example images are shown on the left: upper panel: signal for newly synthesized proteins (red), lower panel: overlay with tubulin staining (green). Scale bar is 20  $\mu$ m. (I) Increasing concentrations of TGX-221 (5  $\mu$ mol/L and 10  $\mu$ mol/L) further reduce protein synthesis rates in FXS LCLs to healthy control levels. ( $n$  (Ctr Untr) = 57,  $n$  (Ctr 5  $\mu$ mol/L) = 57,  $n$  (Ctr 10  $\mu$ mol/L) = 55,  $n$  (FXS Untr) = 59,  $n$  (FXS 5  $\mu$ mol/L) = 55,  $n$  (FXS 10  $\mu$ mol/L) = 58; 3 independent experiments, 2-way ANOVA,  $*P$  (genotype) = 0.001,  $*P$  (treatment) < 0.001,  $*P$  (interaction genotype–treatment) < 0.001; Games-Howell *post hoc* analyses,  $*P = 0.001$ ,  $^{ns(1)}P = 0.966$ ,  $^{ns(2)}P = 0.999$ ). Protein synthesis rates in FXS cells were significantly reduced after treatment with either 5  $\mu$ mol/L or 10  $\mu$ mol/L TGX-221 ( $P$  (Ctr 5/10  $\mu$ mol/L) < 0.001), whereas there was no significant difference between FXS cells treated with 5 and 10  $\mu$ mol/L TGX-221 ( $P$  (5–10  $\mu$ mol/L) = 0.992), or between healthy control cells after treatment ( $P$  (Ctr 5  $\mu$ mol/L) = 0.271;  $P$  (Ctr 10  $\mu$ mol/L) = 0.638). a.u., Arbitrary units; Untr, untreated; ns(1), not significant (comparison 1); ns(2), not significant (comparison 2). B–D:  $\square$ , WT;  $\blacksquare$ , KO; F–I:  $\square$ , Ctr;  $\blacksquare$ , FXS.

tial biomarkers that quantify molecular defects directly caused by the absence of FMRP. This assumption is corroborated by our observation that the underlying pathomechanisms occurring in neurons are recapitulated in peripheral lymphoblastoid cells. We could detect increased and dysregulated protein synthesis in FXS patient lymphoblastoid cells, similar to what we and others have observed in neuronal synaptic fractions and brain slices from *Fmr1* KO mice (1-4,25). Furthermore, we show that PI3K activity and downstream signaling is upregulated in these cells, likewise resembling observations in *Fmr1* KO mice (3,26). We have shown previously that FMRP controls PI3K activity by regulating at least two of its target mRNAs, namely p110 $\beta$  and PIKE-L (3). FMRP limits the expression of these proteins (3,26), leading to increased and stimulus-insensitive PI3K activity, which might underlie dysregulated synaptic protein synthesis in the absence of FMRP (3). Here, we demonstrate that p110 $\beta$  levels are also increased in LCLs from two different patients with FXS, suggesting that the pathological molecular mechanisms that occur in neurons are recapitulated in peripheral lymphocytes.

A previous study has shown that polysomal profiles of several potential FMRP target mRNAs are abnormal in LCLs from patients with FXS, suggesting their dysregulated translation (18). However, to our knowledge, no study has reported dysregulated basal and stimulus-induced general protein synthesis in cells from human patients with FXS so far. The absence of IL-2-induced stimulation of protein synthesis in LCLs from a patient with FXS suggests that an intracellular signaling pathway downstream of IL-2, which regulates protein synthesis, is over-active and insensitive to stimulation in these cells. Interestingly, contrary to the effect in healthy control cells, we observed a significant reduction of protein synthesis rates in patient LCLs upon IL-2 stimulation. At present, we cannot explain this observation, but speculate that

it might be caused by a negative feedback mechanism, which is still functional in the patient cells. Cytokines such as IL-2, play an important role for cell proliferation and survival. The lack of a proper response to these prosurvival stimuli in the absence of FMRP might therefore contribute to the reduced cancer rates that have been reported for patients with FXS (27).

We show that a p110 $\beta$ -selective antagonist can rescue increased protein synthesis in patient LCLs to control levels, reporting a significant interaction between genotype and treatment, which suggests that increased p110 $\beta$ -mediated PI3K activity and downstream signaling underlies the dysregulated protein synthesis in these cells. Furthermore, together with our observation of excess p110 $\beta$ -associated PI3K activity, this suggests that targeting the p110 $\beta$  subunit might be a potential therapeutic strategy for FXS. Of note, our data show that in contrast to p110 $\beta$ , the two other class 1A PI3K catalytic subunits, p110 $\alpha$  and  $\delta$ , are unchanged in LCLs from FXS patients, thereby corroborating the potential benefits of a p110 $\beta$ -targeted therapy in FXS. As mentioned above, previous work has suggested that FMRP also regulates another modulator of PI3K activity, the PI3K enhancer PIKE (3,26). Future studies could analyze whether PIKE is also dysregulated in cells from patients with FXS and thus might serve as valuable therapeutic target. However, in contrast to p110 $\beta$ , no specific antagonists of PIKE are currently available for the use in humans, suggesting that pursuing p110 $\beta$ -specific therapeutic strategies might have a more immediate beneficial effect for patients with FXS.

Previous studies have corroborated the importance of PI3K function for IL-2-induced protein synthesis in T-lymphocytes by showing that a broad-spectrum PI3K antagonist leads to a strong reduction of protein synthesis rates in T-cells cultured in the presence of IL-2 (28). Here, we show that even a high dose of the p110 $\beta$ -subunit selective

antagonist TGX-221 (10  $\mu$ mol/L, 1000 $\times$  over IC<sub>50</sub>) does not significantly affect basal protein synthesis rates in healthy control LCLs. The lack of effect on control cells suggests that under healthy conditions, p110 $\beta$  (or general PI3K) activity might only be required for stimulus-induced protein synthesis. In the future, it will be interesting to examine the effect of p110 $\beta$ -selective antagonists on IL-2-induced protein synthesis in LCLs from healthy controls and FXS patients. An alternative explanation for the absence of an effect of the p110 $\beta$  antagonist on protein synthesis in healthy control cells might be that other class 1 p110 catalytic subunits can compensate for the loss of p110 $\beta$  activity to sustain protein synthesis in normal LCLs. It was shown previously that genetic or pharmacological inhibition of one or more class 1 PI3K catalytic subunits in immortalized leukocytes and fibroblasts leads to functional compensation by the other subunits to preserve cell survival and proliferation (29). In line with this observation, results from cancer research suggest that a monotherapy using single subunit-selective PI3K antagonists might not be efficient to stop tumor growth due to functional compensation by other catalytic subunits (30). This further supports the applicability of therapies targeting p110 $\beta$  in patients with FXS, because it suggests that basic cell functions, such as mitosis and cell survival might not be affected by p110 $\beta$ -selective antagonists.

Our observation that neuronal disease mechanisms of FXS, such as dysregulated PI3K-mediated protein synthesis, are detectable in nonneuronal, peripheral cell lines from human patients has two important implications: firstly, lymphoblastoid cells and peripheral blood lymphocytes might be suitable as a biomarker tool for FXS that detects underlying pathomechanisms, and secondly, they may thus be used for drug screens to identify disease-targeted therapeutics. This hypothesis is corroborated by our study showing that a p110 $\beta$ -selective antagonist, TGX-221, can rescue excess pro-



tein synthesis not only in synaptic fractions from the FXS mouse model, but also in patient lymphoblastoid cells. Lymphoblastoid cell lines are a valuable and efficient tool for personalized drug screens to identify therapeutics in specific patients. They are easy to obtain and are a virtually unlimited source of patient material. Of note, two of the here described assays, the PI3K activity ELISA and the Click-iT protein synthesis assay, are colorimetric or fluorescent, respectively, and thus suitable for larger-scale applications needed to perform drug screens.

Quantification of PI3K signaling and protein synthesis rates in peripheral lymphocytes might also have a broader applicability as a biomarker beyond FXS, for example, for autism research. Autism spectrum disorders (ASDs) are a highly variable group of disorders. The majority is idiopathic, and only a few monogenic defects have been shown to lead to autism (31). FXS is the most frequent monogenic ASD, but of note, it is not the only one that is characterized by dysregulated signaling through PI3K/mTOR. Another example is tuberous sclerosis, which is caused by mutations or deletions in the tuberous sclerosis complex 1/2 (*TSC1/2*). *TSC1/2* regulates mTOR signaling, and approximately 25–50% of patients with tuberous sclerosis develop ASD (32,33). Furthermore, mutations in phosphatase and tensin homologue on chromosome 10 (*PTEN*) have been associated with several forms of ASD (34). *PTEN* regulates the PI3K/mTOR pathway by dephosphorylating phosphoinositide-(3,4,5)-triphosphate ( $PIP_3$ ), the product of PI3K. Apart from these known monogenic causes for ASD, a considerable number of chromosomal copy number variations associated with ASDs were shown to affect genes within the PI3K/mTOR pathway (35). The high frequency of PI3K/mTOR defects in ASDs with known underlying gene defects suggests that dysregulated PI3K/mTOR signaling and/or protein synthesis might also be the cause of other, so far

idiopathic, ASDs. Interestingly, a recent study showed that a mouse model for Rett syndrome, a rare form of autism caused by mutations in the gene encoding the epigenetic regulator methyl CpG-binding protein 2 (MeCP2), displays reduced PI3K/mTOR signaling and protein synthesis (36), suggesting that mutations or defects in other pathways might have an effect on PI3K/mTOR signaling. Moreover, aberrant neuronal protein synthesis was hypothesized to be a shared pathomechanism of several inherited ASDs (37). Taken together, this suggests that the here described assays detecting aberrant PI3K/mTOR signaling as well as dysregulated protein synthesis in peripheral patient cells might also be useful biomarker tools for other ASDs apart from FXS. In particular, such assays could be used for screens using lymphoblastoid cell lines from patients with idiopathic ASD to identify those who would qualify for a PI3K/mTOR-based therapy. Several collections of ASD lymphoblastoid cell lines are already available for researchers, for example, from the Simons Simplex Collection (SSC) or the Autism Genetic Research Exchange (AGRE).

## CONCLUSION

Our results suggest that quantitative analysis of PI3K activity and protein synthesis rates in LCLs from patients with FXS may be a valuable tool for drug screens to identify more potent therapeutic strategies for FXS and other ASDs that directly target underlying mechanisms. Together with our previous work demonstrating that a broad spectrum PI3K inhibitor can rescue several phenotypes in *Fmr1* KO mouse neurons (3), the current study also suggests that PI3K subunit-selective antagonists might be a valuable therapeutic treatment for FXS. Several different forms of cancers are caused by multiple mutations within the PI3K signaling pathway, and subunit-selective PI3K inhibitors have been developed and are currently being tested for the treatment

of specific tumors (30). In the future, FXS and autism research could greatly benefit from these developments in the field of cancer research, where PI3K targeting drugs are already being tested for their safety and applicability in human patients.

## ACKNOWLEDGMENTS

The authors would like to thank M Kim and A Poopal for excellent technical assistance, and J Mowrey for valuable advice on LCL culturing. Lymphoblastoid cell lines from FXS patients and healthy controls were a kind gift from S Warren (Emory University). The authors thank S Warren for helpful discussions. The authors thank S Swanger for critically reading the manuscript, and all members of the Bassell lab for helpful discussions. This work was supported by a postdoctoral fellowship from FRAXA (to C Gross), the NIH Grant MH085617 (to GJ Bassell), the Emory/Baylor Fragile X Center Grant 3P30HD024064 (to GJ Bassell), and a Suzanne and Bob Wright Trailblazer Award from Autism Speaks (to GJ Bassell).

## DISCLOSURE

The authors are coinventors on patent application PCT/US2010/055387, which suggests the use of (1) PI3K antagonists as a therapeutic treatment for fragile X syndrome and other autism spectrum disorders and (2) PI3K activity as a biomarker for these diseases.

## REFERENCES

- Osterweil EK, Krueger DD, Reinhold K, Bear MF. (2010) Hypersensitivity to mGluR5 and ERK1/2 leads to excessive protein synthesis in the hippocampus of a mouse model of fragile X syndrome. *J. Neurosci.* 30:15616–27.
- Qin M, Kang J, Burlin TV, Jiang C, Smith CB. (2005) Postadolescent changes in regional cerebral protein synthesis: an in vivo study in the *Fmr1* null mouse. *J. Neurosci.* 25:5087–95.
- Gross C, et al. (2010) Excess phosphoinositide 3-kinase subunit synthesis and activity as a novel therapeutic target in fragile X syndrome. *J. Neurosci.* 30:10624–38.
- Muddashetty RS, Kelic S, Gross C, Xu M, Bassell GJ. (2007) Dysregulated metabotropic glutamate receptor-dependent translation of AMPA receptor and postsynaptic density-95 mRNAs at

- synapses in a mouse model of fragile X syndrome. *J. Neurosci.* 27:5338–48.
5. Bear MF, Dolen G, Osterweil E, Nagarajan N. (2008) Fragile X: translation in action. *Neuropsychopharmacology.* 33:84–7.
  6. Bassell GJ, Warren ST. (2008) Fragile X syndrome: loss of local mRNA regulation alters synaptic development and function. *Neuron.* 60:201–14.
  7. Nosyreva ED, Huber KM. (2006) Metabotropic receptor-dependent long-term depression persists in the absence of protein synthesis in the mouse model of fragile X syndrome. *J. Neurophysiol.* 95:3291–5.
  8. Volk LJ, Pfeiffer BE, Gibson JR, Huber KM. (2007) Multiple Gq-coupled receptors converge on a common protein synthesis-dependent long-term depression that is affected in fragile X syndrome mental retardation. *J. Neurosci.* 27:11624–34.
  9. Weiler IJ, et al. (2004) Fragile X mental retardation protein is necessary for neurotransmitter-activated protein translation at synapses. *Proc. Natl. Acad. Sci. U.S.A.* 101:17504–9.
  10. Gross C, Berry-Kravis EM, Bassell GJ. (2012) Therapeutic strategies in fragile X syndrome: dysregulated mGluR signaling and beyond. *Neuropsychopharmacology.* 37(1):178–95.
  11. Krueger DD, Bear MF. (2011) Toward fulfilling the promise of molecular medicine in fragile X syndrome. *Ann. Rev. Med.* 62:411–29.
  12. Bolduc FV, Bell K, Cox H, Broadie KS, Tully T. (2008) Excess protein synthesis in Drosophila fragile X mutants impairs long-term memory. *Nat. Neurosci.* 11:1143–5.
  13. Jacquemont S, et al. (2011) Epigenetic modification of the FMR1 gene in fragile X syndrome is associated with differential response to the mGluR5 antagonist AFQ056. *Sci. Translat. Med.* 3:64ra61.
  14. Berry-Kravis E, et al. (2008) Open-label treatment trial of lithium to target the underlying defect in fragile X syndrome. *J. Dev. Behav. Pediatr.* 29:293–302.
  15. Weng N, Weiler IJ, Sumis A, Berry-Kravis E, Greenough WT. (2008) Early-phase ERK activation as a biomarker for metabolic status in fragile X syndrome. *Am. J. Med. Genet. B. Neuropsychiatr. Genet.* 147B:1253–7.
  16. Erickson CA, et al. (2011) Open-label riluzole in fragile X syndrome. *Brain Res* 1380:264–270.
  17. Committee for the Update of the Guide for the Care and Use of Laboratory Animals, Institute for Laboratory Animal Research, Division on Earth and Life Studies. (2011) *Guide for the Care and Use of Laboratory Animals*. 8th edition. Washington (DC): National Academies Press. [cited 2012 Apr 17]. Available from: <http://oacu.od.nih.gov/regs/>
  18. Brown V, et al. (2001) Microarray identification of FMRP-associated brain mRNAs and altered mRNA translational profiles in fragile X syndrome. *Cell* 107:477–87.
  19. Feng Y, et al. (1997) FMRP associates with polyribosomes as an mRNP, and the I304N mutation of severe fragile X syndrome abolishes this association. *Mol. Cell* 1:109–18.
  20. Lugenbeel KA, Peier AM, Carson NL, Chudley AE, Nelson DL. (1995) Intragenic loss of function mutations demonstrate the primary role of FMR1 in fragile X syndrome. *Nat. Genet.* 10:483–5.
  21. Ye K, et al. (2000) PIKE: A nuclear GTPase that enhances PI3Kinase activity and is regulated by protein 4.1N. 103:919–930.
  22. Altman A, Mustelin T, Coggeshall KM. (1990) T lymphocyte activation: a biological model of signal transduction. *Crit. Rev. Immunol.* 10:347–91.
  23. Dieterich DC, Link AJ, Graumann J, Tirrell DA, Schuman EM. (2006) Selective identification of newly synthesized proteins in mammalian cells using bioorthogonal noncanonical amino acid tagging (BONCAT). *Proc. Natl. Acad. Sci. U.S.A.* 103:9482–7.
  24. Jackson SP, et al. (2005) PI 3-kinase p110beta: a new target for antithrombotic therapy. *Nat. Med.* 11:507–14.
  25. Dolen G, et al. (2007) Correction of fragile X syndrome in mice. *Neuron.* 56:955–62.
  26. Sharma A, et al. (2010) Dysregulation of mTOR signaling in fragile X syndrome. *J. Neurosci.* 30:694–702.
  27. Schultz-Pedersen S, Hasle H, Olsen JH, Friedrich U. (2001) Evidence of decreased risk of cancer in individuals with fragile X. *Am. J. Med. Gen.* 103:226–30.
  28. Cornish GH, Sinclair LV, Cantrell DA. (2006) Differential regulation of T-cell growth by IL-2 and IL-15. *Blood.* 108:600–8.
  29. Foukas LC, Berenjano IM, Gray A, Khwaja A, Vanhaesebroeck B. (2010) Activity of any class IA PI3K isoform can sustain cell proliferation and survival. *Proc. Natl. Acad. Sci. U.S.A.* 107:11381–6.
  30. Markman B, Atzori F, Perez-Garcia J, Tabernero J, Baselga J. (2010) Status of PI3K inhibition and biomarker development in cancer therapeutics. *Ann. Oncol.* 21:683–91.
  31. Kotulska K, Józwiak S. (2011) Autism in monogenic disorders. *Eur. J. Paediatr. Neurol.* 15:177–80.
  32. Smalley SL. (1998) Autism and tuberous sclerosis. *J. Autism Dev. Disord.* 28:407–14.
  33. Wiznitzer M. (2004) Autism and tuberous sclerosis. *J. Child Neurol.* 19:675–9.
  34. McBride KL, et al. (2010) Confirmation study of PTEN mutations among individuals with autism or developmental delays/mental retardation and macrocephaly. *Autism Res.* 3:137–41.
  35. Cusco I, et al. (2009) Autism-specific copy number variants further implicate the phosphatidylinositol signaling pathway and the glutamatergic synapse in the etiology of the disorder. *Hum. Mol. Genet.* 18:1795–804.
  36. Ricciardi S, et al. (2011) Reduced AKT/mTOR signaling and protein synthesis dysregulation in a Rett syndrome animal model. *Hum. Mol. Genet.* 20:1182–96.
  37. Kelleher RJ, 3rd, Bear MF. (2008) The autistic neuron: troubled translation? *Cell* 135:401–6.